Novel chitosan-cellulose hydrogel adsorbents for lead adsorption

Nan Li and Renbi Bai*
Department of Chemical and Biomolecular Engineering
National University of Singapore
10 Kent Ridge Crescent
Singapore 119260
*Fax: (65) 6779 1936; E-mail: chebairb@nus.edu.sg

Abstract

In this study, we examined the properties of chitosan-cellulose hydrogel beads as an adsorbent and its application for lead ion adsorption. Chitosan was blended with cellulose to improve the mechanical strength of chitosan hydrogel beads and the chitosan-cellulose hydrogel beads were cross-linked with ethylene glycol diglycidyl ether (EGDE) to enhance their acid-resistant ability. Scanning electron microscopic (SEM) observation also showed that the crosslinking reaction resulted in the chitosan-cellulose hydrogel beads having porous surface structure. Batch adsorption experiments indicated that both the chitosan-cellulose and the crosslinked chitosan-cellulose hydrogel beads had high adsorption capacities for lead ion removal although the adsorption performances were pH-dependent. The adsorption isotherm of chitosan-cellulose beads and crosslinked chitosan-cellulose beads can be well fitted to the Freundlich model. The kinetic adsorption data obeyed the Fickan's law and suggested an intraparticle-diffusion-controlled adsorption process. X-ray photoelectron spectroscopy (XPS) revealed that the amine groups on chitosan were involved in the surface complexation for lead ion adsorption.

Keywords: Chitosan-cellulose beads; EDGE crosslinking; Lead adsorption; Surface interaction; Mechanisms.

1. Introduction

Heavy metal contamination of various water resources is of great concern because of the toxic effect to the human beings and other animals and plants in the environment. The major sources of heavy metal pollutants are usually from many industries, including mining, metal plating, electric device manufacturing, and so on. For example, lead is extensively used in the electrical industry, and in the manufacture of fungicides and anti-fouling paints [1]. Lead could cause harmful, acute and even fatal effect when a large dosage is ingested [2]. Since heavy metal ions are not biodegradable, they are usually removed physically or chemically from the contaminated water. Conventional methods that have been used to remove heavy metal ions from various industrial effluents usually include chemical precipitation, membrane separation, ion exchange, evaporation, and electrolysis, etc. and are often costly or ineffective, especially in removing heavy metal ions from dilute solutions [2, 3]. One of the new developments for metal removal in recent years is to use biosorption. Many materials of biological origins have been studied as adsorbents to remove various heavy metal ions from water and industrial effluents [3]. Particularly, chitosan, a derivative from N-deacetylation of chitin - a naturally occurring polysaccharide from crustacean and

fungal biomass, has been found to be capable of chemically or physically adsorbing various heavy metal ions, including lead, vanadium, platinum, silver, cadmium, chromium, and lead [1,4,5,6,7,8]. Chitosan may also be cheaply obtained from chitin which is the second most naturally abundant biopolymer (next to cellulose) and is readily available from seafood-processing wastes.

Traditionally, chitosan has been used in the form of flakes or powder in metal adsorption. Because raw chitosan can be characterized as a crystallized polymer, metal ions could only be adsorbed onto the amorphous region of the crystals [9]. Progress has been made to produce chitosan hydrogel beads to improve the adsorption capacity of chitosan by reducing the crystallinity through the gel formation process [6], and also provide the potential for regeneration and reuse of the hydrogel beads after metal adsorption [4,6,10,11]. The major material limitation of the hydrogel beads is however in their poor acidic resistance and mechanical strength. Attempts have been made to improve the chemical stabilities of the hydrogel beads in acidic conditions by chemical crosslinking of the surface with crosslinking agents, such as glutaricdialdehyde (GA), ethylene glycol diglycidyl ether (EGDE), and epichlorhydrine [4]. Chemical crosslinking reaction was found to be able to reduce the solubility of chitosan hydrogel beads in aqueous solutions of low pH values. On the other hand, polymer blending has increasingly been used as a method for providing polymeric materials with desirable properties. Jin and Bai [4] studied lead adsorption with chitosan/PVA hydrogel beads and found that the blending of PVA (polyvinyl alcohol) in chtiosan improved the mechanical strength of the hydrogel beads.

In this paper, we report the study of using chitosan-cellulose hydrogel beads for lead adsorption. The interest in using cellulose as a blending polymer for chitosan arises from two facts: (a) cellulose is the most abundant natural biopolymer with relatively strong mechanical strength of up to $1GN/m^2$ (10,000Mpa) [12], and (b) cellulose has similar chemical structures as chitosan, providing the possibility of producing a homogeneous blend that combine the unique properties of chitosan and the good availability of cellulose to make chitosan-cellulose hydrogel beads as an adsorbent for metal adsorption. The study included the synthesis of the chitosan-cellulose hydrogel beads, chemical crosslinking of the chitosan-cellulose hydrogel beads with EGDE, and the examination of the adsorption performance and mechanisms with the hydrogel beads for lead removal. A series of batch adsorption experiments under various solution pH values and initial lead ion concentrations was conducted and various analyses, such as zeta potential measurements, X-ray photoelectron spectroscopy (XPS), were performed. The results are presented below.

2. Experimental work

2.1 Materials and chemicals

Chitosan flakes (85% deacetylated) and cellulose powder (20 μm) were purchased from Sigma Co. Ethylene Glycol Diglycidyl Ether (EGDE), lead (II) standard solution (1000 mg/l), and acetic acid were provided by Merck. All other chemicals were of reagent grade purity and deionized (DI) water was used to prepare all solutions.

2.2 Preparation of chitosan-cellulose hydrogel beads

A 2 g amount of chitosan flakes was added into 100 ml 2 %(w/w) acetic acid (denoted as HAc) in a beaker and the contents in the beaker were mixed on a hot plate stirrer at 70 ^{o}C and 200 rpm for 6 h. Then, a 2 g amount of cellulose powder was added into the chitosan solution and the mixing was continued for another 6 h at room temperature (22-23 ^{o}C) and 200 rpm on the stirrer. The blended solution was then injected in droplets into a 1 M NaOH solution to form hydrogel beads through a vibration nozzle system (Nisco Encapsulation Unit, LIN-0018, with nozzle size of 300 μm). The chitosan-cellulose hydrogel beads were allowed to stay in the NaOH solution with slow stirring for another 12 h for hardening. The hardened beads were finally separated from the NaOH solution and were washed with DI water in a large beaker until the solution pH became the same as that of the fresh DI water. Then, the beads were stored in DI water for further use.

Some experiments involved in the crosslinking of the chitosan-cellulose hydrogel beads with ethylene glycol diglycidyl ether (EGDE). To do that, the beads in stock were taken out from DI water and removed the attached surface water by placing them on a few pieces of filter papers for several min. Then, 25 ml of the chitosan-cellulose beads was suspended into 25 ml of DI water in a beaker, with the pH being adjusted to 12 by the addition of 0.1 M NaOH solution. After 5 min, a 0.4 g amount of EGDE solution was added into the beaker and the crosslinking reaction was allowed to proceed at 70 ^{o}C for 6 h in a thermostatic water bath with continuous agitation. Finally, the mixture was cooled down to room temperature, and the crosslinked chitosan-cellulose beads were washed in an ultrasonic bath with sufficient DI water until the pH of the solution became around 6-6.5 (the same as the fresh DI water). The beads were then stored in DI water for further use.

2.3 Zeta potential measurement

Zeta potentials are often used as an important parameter in analyzing the electrostatic surface interaction in adsorption. To estimate the zeta potentials of the chitosan-cellulose hydrogel beads, about a 0.1 g amount of the dried chitosan-cellulose hydrogel beads (crosslinked or non-crosslinked) was ground into powder and suspended into 100 ml of DI water. The mixture was sonicated first for 4 h, followed by stirring for another 24 h, and then settled for 12 h. Samples were taken from the supernatants (which had colloidal fragments from the chtiosan-cellulose beads in it) and were used for zeta potential analysis. Before the analysis, each sample was distributed into several vials. The pH values of the sample in each of the vials were adjusted with 0.1 M HCl or 0.1 M NaOH solution to a desired level. A Zeta-Plus4 instrument (Brookhaven Corp., USA) was used to measure the zeta potentials of all the samples. Zeta potentials so determined from the fragments in the samples were assumed to represent the zeta potentials of the chitosan-cellulose hydrogel beads in solutions of the same pH values [13].

2.4 Adsorption experiments

2.4.1 Lead adsorption at different solution pH

To study the effect of solution pH on lead adsorption on chitosan-cellulose hydrogel beads, lead solutions with an initial concentration of 30 mg/l were prepared by diluting the 1000 mg/l standard lead solution with DI water, and, then, the pH values of the solutions were adjusted to a value in the range of 3 to 9, respectively, with 0.1 M NaOH or 0.1 M HCl. A certain amount of chitosan-cellulose beads was taken out from the stock and removed the

surface water by placing them on a filter paper for a few min. Then, about a 0.1 g amount of the chitosan-cellulose beads was weighed and added, respectively, into a number of 25 ml plastic bottles, each of them contained 10 ml of the lead solutions of different solution pH values mentioned above. The contents in the bottles were stirred in an orbital shaker at 200 rpm and room temperature (22-23 ^{o}C) for adsorption to proceed. The pH of the solutions in each flask was not controlled during the adsorption process (in order not to introduce any additional ions into the solution). After 48 h, samples were taken from the bottles for the determination of the final lead concentrations in the solutions. Lead concentrations in the samples were analyzed using an Inductively Coupled Plasma-Optical Emission Spectrometer (ICP-OES, Perkin Elmer Optima 3000DV). Both crosslinked and non-crosslinked chitosan-cellulose beads were studied. The amount of adsorption, q (mg/g), was calculated from the following equation:

$$q = \frac{(C_o - C_e)V}{m} \quad (1)$$

where C_0 (mg/l) and C_e (mg/l) are the initial and final lead concentrations of the solution in each bottle, respectively, V (l) is the volume of the lead solution in each bottle, and m (g) is the weight of chitosan-cellulose hydrogel beads added into each bottle.

2.4.2 Adsorption equilibrium study

The experiments were conducted with solutions of lead concentrations ranging from 5 to 100 mg/l but of the same initial solution pH value of 6. About a 0.1 g amount of the chitosan-cellulose beads was added, respectively, into 5 ml of each type of the solutions with different initial lead concentrations in a number of 25 ml plastic bottles. The mixtures in the bottles were stirred on an orbital shaker operated at 200 rpm and room temperature for 7 days (The pH of the solutions was again not adjusted during the adsorption process). The initial and final lead concentrations in the solutions in each of the bottles were determined using an ICP-OES. Similar experiments were carried out for both the chitosan-cellulose hydrogel beads and the crosslinked chitosan-cellulose hydrogel beads. The adsorption capacities were also calculated using Eq.(1).

2.4.3 Kinetic adsorption experiments

Kinetic study used a solution of an initial pH 6 and an initial lead ion concentration of 15 mg/l. A 12.5 g amount of the chitosan-cellulose beads (non-crosslinked or crosslinked) was added into 500 ml of the lead solution in an one-liter flask. The mixture in the flask was shaken on an orbit shaker operated at 200 rpm and room temperature for a period of up to 24 h or until adsorption equilibrium was established. The histories of lead ion concentration in the solutions were determined by taking and analyzing solution samples periodically. The adsorbed amounts of lead ions per unit weight of the hydrogel beads at time t_i, $q(t_i)$ (mg/g), was calculated from the mass balance equation as:

$$q(t_i) = \frac{\sum_{i=1}^{n}(C_{t_{i-1}} - C_{t_i})V_{t_{i-1}}}{m} \quad (2)$$

where C_{t_0} (= C_0) and C_{t_i} (mg/l) are the initial lead concentration and the lead concentrations at time t_i, respectively; V_{t_i} is the volume of the solution at time t_i (Samples taken for lead concentration analysis were not returned to the flask), and *m* is the weight of the hydrogel beads added into the flask.

2.5. Surface morphology observation with Scanning Electron Microscope (SEM)

The chitosan-cellulose and the crosslinked chitosan-cellulose hydrogel beads were put into a desiccator at 10 mTorr vacuum and room temperature for 72 h to remove excess moisture. The surface morphology was observed using a JEOL scanning electron microscope (JSM-5600LV) with a high resolution of 3.5 nm under high vacuum. Samples were platinum-coated by a vacuum electric sputter coater (JEOLJFC-1300) to a thickness of at least 500 angstroms before glue-mounted onto the sample stud for the SEM scan.

2.6 X-ray Photoelectron Spectroscopy (XPS)

XPS analyses of the chitosan-cellulose and the crosslinked chitosan-cellulose hydrogel beads before and after lead adsorption were made on a VGESCALAB MKII spectrometer with an Al Kα X-Ray source (1486.6eV of photons), following a similar procedure described by Bai et al. [14]. The XPS spectra peaks were decomposed into subcomponents by fixing the 0% Lorentzian-Gaussian Curve-fitting program with a linear background to the spectra through an XPSpeak 4.1 software package. The full width half maximum was maintained at 1.4. The calibration of the binding energy (BE) of the spectra was performed with the C 1s peak of the aliphatic carbons at 284.6 eV.

3. Results and discussion

3.1 Surface morphology

Macroscopically, the prepared chitosan-cellulose hydrogel beads were reasonably good in spherical shape; see Fig.1. Both the chitosan-cellulose and the crosslinked chitosan-cellulose hydrogel beads had a milk-white color with a mean diameter of about 3.1 mm. The SEM images in Fig.2 clearly show that the addition of cellulose into chitosan made the surface of the chitosan-cellulose hydrogel beads much denser than that of the chitosan hydrogel beads, and the crosslinking reaction with EGDE also made the surface of the chitosan-cellulose hydrogel beads very porous. It has been reported that the crosslinking agent EGDE was prone to react with amine groups instead of hydroxyl groups [5]. Therefore, the porous structure of the crosslinked chitosan-cellulose hydrogel beads may be formed due to the bridging connection of EGDE between different amine groups in chitosan through intra-molecular and/or inter-molecular crosslinking. FTIR analysis (spectra are not shown here) of the chitosan-cellulose hydrogel beads and the crosslinked chitosan-cellulose hydrogel beads showed that the peaks representing the amine groups shifted and became weaker after the crosslinking reaction, suggesting that crosslinking reaction with EGDE indeed involved in the amine groups in chitosan.

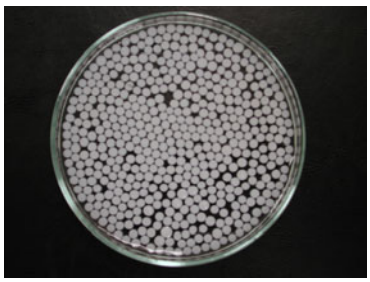

Figure 1 The macroscopic shape of the chitosan-cellulose hydrogel beads

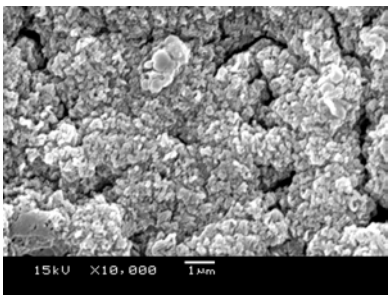

(a)

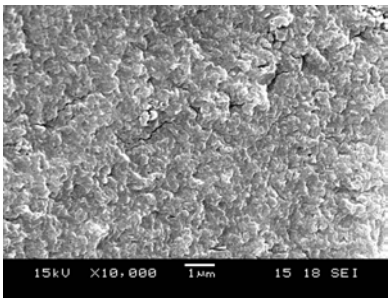

(b)

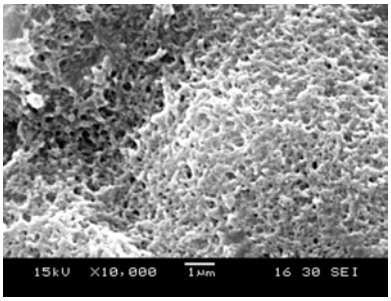

(c)

Figure 2 SEM images showing the surface morphologies of the chitosan, chitosan-cellulose and crosslinked Chitosan-Cellulose hydrogel Beads: (a) Chitosan, (b) Chitosan-cellulose, (c) Crosslinked chitosan-cellulose

3.2 Zeta potentials

The zeta potentials of the chitosan-cellulose and the crosslinked chitosan-cellulose beads under different solution pH values are shown in Fig. 3. It is observed that chitosan-cellulose beads had positive zeta potentials in acidic solutions and negative zeta potentials in basic solutions, with a point of zero zeta potential at about pH 6.7. The pK_a value of the amine group in chitosan molecule has been known to be dependent on the extent of deacetylation. Park et al. reported that the pK_a was 6.1 when $\alpha < 0.72$ and 6.7 when $\alpha > 0.72$ [15]. The α value of chitosan used in this study was greater than 0.85, and, hence, the point of zero zeta potential at about pH 6.7 for the chitosan-cellulose beads was essentially the same as the pK_a value of the amino group in chitosan [4,15,16]. From the electrostatic interaction point of view, the positive zeta potentials of the chitosan-cellulose beads under acidic solution conditions would favor the adsorption of negatively charged species and the negative zeta potentials of the beads under basic solution conditions may enhance the adsorption of positively charged species. The crosslinking reaction is observed to slightly reduce the positive zeta potentials of the beads at pH<6.7. Since the positive zeta potentials of the beads may partially result from the protonation of the amine groups in chitosan, the reduction of the positive zeta potentials of the crosslinked chitosan-cellulose beads may again indicates that some of the amine groups on the chitosan-cellulose beads were consumed or sheltered by the cross-linking reactions.

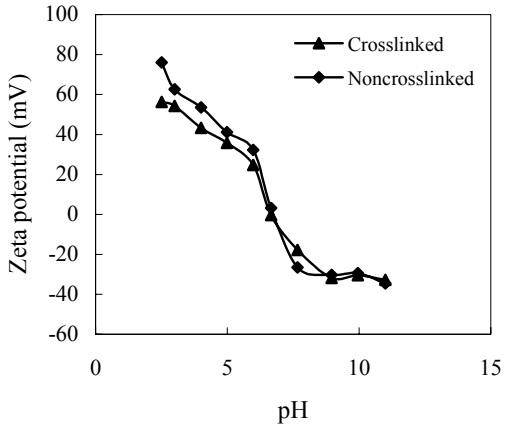

Figure 3 Zeta potentials of the chitosan-cellulose and the crosslinked chitosan-cellulose beads at different solution pH values

3.3 Effect of pH on lead adsorption

Fig.4 shows the amounts of lead ion adsorption on the chitosan-cellulose and the crosslinked chitosan-cellulose beads in solutions of initial pH values from 3 to 9 (lead ions mainly existed as Pb^{2+} in this pH range). In general, the adsorption capacities increased with the increase of the solution pH values for both the chitosan-cellulose beads and the crosslinked chitosan-cellulose beads and the maximum adsorption capacity reached about 50-60 mg/g in this case. It is also observed that the chitosan-cellulose beads always had greater adsorption capacities than the crosslinked chitosan-cellulose beads in the pH range studied.

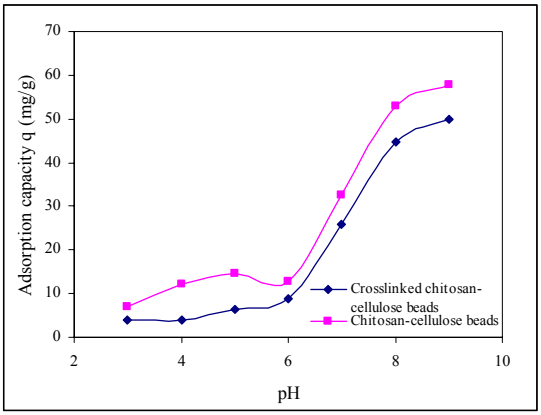

Figure 4 Effect of initial solution pH values on lead adsorption capacities on the chitosan-cellulose and the crosslinked chitosan-cellulose beads (initial lead ion concentration in the solution: 30 mg/l)

As mentioned earlier, the zeta potentials of both the chitosan-cellulose and the crosslinked chitosan-cellulose beads were positive at pH<6.7 and negative at pH>6.7. The electrostatic interaction between the two types of beads and the lead ions to be adsorbed would be repulsive at pH<6.7 but become attractive at pH>6.7. The repulsive electrostatic interaction at pH<6.7 may hinder lead ions in the bulk solution from approaching the surfaces of the beads for adsorption to take place. However, the electrostatic repulsion decreased with the increase of the solution pH. This probably explains the observed increase of the adsorption capacities with solution pH from 3 up to 6.7. At pH above 6.7, the attractive electrostatic interaction between the beads and the lead ions to be adsorbed may favor the adsorption to take place, but the adsorption capacities in Fig.4 are not observed to further increase with solution pH at pH > 6.7. The changes of the adsorption performance with solution pH in Fig.4 may be more clearly explained from the acid-base properties of the beads (adsorbents). Eqs.(3), (4), and (5) below can be used to show some of the major reactions that may take place in the solution:

$$-NH_2 + H^+ \leftrightarrow -NH_3^+ \quad (3)$$

$$-NH_2 + Pb^{2+} \rightarrow -NH_2Pb^{2+} \quad (4)$$

$$-NH_2 + OH^- \leftrightarrow -NH_2OH^- \quad (5)$$

Eq.(3) indicates the protonation and deprotonation reactions of the amine groups of chitosan in the solution, Eq.(4) shows the formation of surface complexes of lead ions with the amine groups, and Eq.(5) describes the binding of OH^- from the solution with the amine groups through hydrogen bond [4]. At lower solution pH values, the reaction in Eq.(3) favored the protonation of the amine groups to form $–NH_3^+$. Since more $–NH_2$ groups were converted to $–NH_3^+$, there were only fewer $–NH_2$ sites available on the beads' surfaces for lead adsorption through Eq.(4). In addition, the formation of more $-NH_3^+$ sites on the surfaces increased the electrostatic repulsion between the lead ions and the surfaces of the beads. All these effects would result in the reduction of lead ion adsorption on the beads with decreasing solution pH values. In comparison with the adsorption capacities of the chitosan-cellulose beads, the significant reductions in lead ion adsorption on the crosslinked chitosan-cellulose beads at pH below about 7 (see Fig.4) can be attributed to the fact that the total number of $–NH_2$ and $–NH_3^+$ groups on the crosslinked chitosan-cellulose beads was much smaller (due to the

crosslinking reaction which consumed some of these groups) and the reaction in Eq.(3) had dramatic impact on the number of $-NH_2$ available for lead ion adsorption through Eq.(4). On the other hand, with the increase of solution pH values, the reaction in Eq.(3) proceeded to the left side and increased the number of $-NH_2$ sites on the surfaces of the beads for lead adsorption through Eq.(4), thus increasing the adsorption capacities. At higher solution pH values, the reaction in Eq.(5) may proceed. This reaction on one hand can reduce the adsorption of lead ions through surface complexation in Eq.(4), but on the other hand may increase the adsorption of lead ions on the beads through electrostatic attractions (non-specific or physical adsorption).

3.4 Adsorption isotherms

Adsorption isotherms describe how adsorbates interact with adsorbents and are important in optimizing the use of adsorbents. The equilibrium adsorption data of lead ions on the chitosan-cellulose beads and the crosslinked chitosan-cellulose beads are shown in Fig.5. The results clearly indicate that, with the increase of initial lead concentrations, the adsorption capacities of both the chitosan-cellulose beads and the crosslinked chitosan-cellulose beads increased significantly, even though the crosslinked chitosan-cellulose beads exhibited lower adsorption capacities.

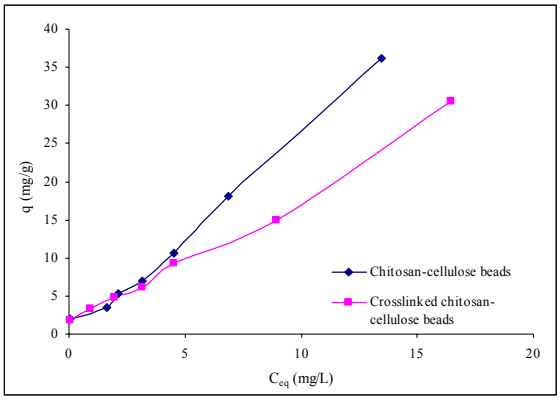

Figure 5 Adsorption capacities of lead ions on the chitosan-cellulose and the crosslinked chitosan-cellulose beads at various initial lead concentrations (initial solution pH = 6)

As shown in Fig.2, the crosslinked chitosan-cellulose beads had porous structures. Hence, the homogeneous surface conditions required by the Langmuir isotherm model may not be met. In addition, the adsorption of lead ions on the crosslinked chitosan-cellulose beads may not follow the monolayer adsorption pattern.

The experimental data in Fig.5 may be analyzed with the Freundlich isotherm model which in its linearized form is:

$$\log q_e = \frac{1}{n}\log C_e + \log P \qquad (6)$$

where P is a constant representing the adsorption capacity (mg/g)(L/mg)^n, and n is a constant depicting the adsorption intensity (dimensionless). The plot of log q_e versus log C_e for the experimental data in Fig.5 is shown in Fig.6. It illustrates that lead adsorption on both the chitosan-cellulose beads and the crosslinked chitosan-cellulose beads obeys the

Freundlich isotherm model reasonably well. The values of the Freundlich model constants P and n are found to be 0.925 and 2.166 for the chitosan-cellulose beads and 1.296 and 2.991 for the crosslinked chitosan-cellulose beads. The greater n for the crosslinked chitosan-cellulose beads indicates that the driving force for lead adsorption for crosslinked chitosan-cellulose beads is greater. However, similar P values for the two types of beads show that the affinity of lead ions for the beads is comparable. The Freundlich model is based on an assumption of adsorption on heterogenerous surfaces and also possibly in multi-layer adsorption pattern. The correlation coefficients in the model fitting in Fig.6 are found to be R^2=0.9941 and R^2=0.9732 respectively for the chitosan-cellulose beads and the crosslinked chitosan-cellulose beads. It is clear that lead ion adsorption on the two types of beads can both well described by the Freundlich model. The analysis hence confirms that the chitosan-cellulose beads and crosslinked chitosan-cellulose beads have heterogeneous surface properties.

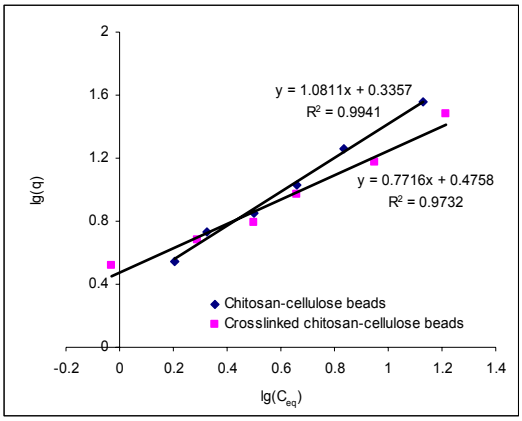

Figure 6 Illustration of the experimental adsorption isotherm data presented in terms of the Freundlich models, respectively, for lead ion adsorption on the chitosan-cellulose and the crosslinked chitosan-cellulose beads (pH = 6)

3.5 Adsorption kinetics

The kinetics of adsorption is to establish the time course of lead uptake on the beads. It is also desirable to examine whether the behavior of lead adsorption on the beads can be described by a theoretical model that is predictive [17,18]. The typical experimental results of lead adsorption on the two types of beads versus adsorption time are shown in Fig.7. Although the chitosan-cellulose beads had greater amount of adsorption than the crosslinked chitosan-cellulose beads, the dynamic behavior of lead adsorption on both types of beads followed a similar change pattern consisting of an initial rapid step and then a second slow step. The adsorption kinetics of the crosslinked chitosan-cellulose beads was however much faster than the chitosan-cellulose beads. It is observed that the adsorption equilibrium was reached at about 7 h for the crosslinked chitosan-cellulose beads but took about 15 h for the chitosan-cellulose beads, possibly due to their higher adsorption capacity. The fast adsorption velocity of the crosslinked chitosan-cellulose beads is probably due to its three dimensional structures as shown in Fig. 2. This porous network structure is favorable for the adsorption in quick diffusion rate and small external resistance. It is easier for lead ions to go through the pore and access the internal binding sites of the sorbent. Therefore,

the external diffusion thickness is very small. In addition, the diffusion rate is also enhanced by the porous structure of crosslinked chitosan-cellulose beads.

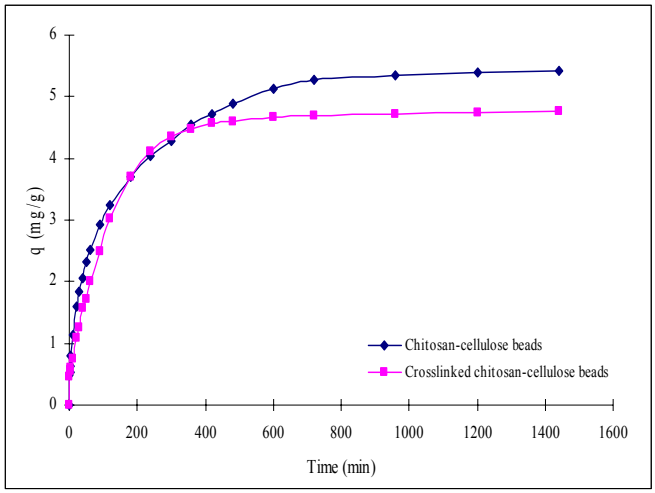

Figure 7 Typical kinetic adsorption results of lead ions on the two types of hydrogel beads (initial solution pH = 6, initial lead ion concentration = 15 mg/l, amount of adsorbent = 12.5 g, and volume of solution = 500 ml)

The adsorption of lead ions on the beads may be considered to consist of two processes: (a) the transport of lead ions from the bulk solution to the surfaces of the beads (including external and/or intraparticular diffusions), and (b) the attachment of lead ions to the active adsorption sites on the surfaces of the beads. In the initial stage, the surfaces of the beads were relatively free of lead ions and the lead ions that arrived at the beads' surfaces may attach instantly to the adsorptive sites on the beads' surfaces. Hence, the adsorption rate may be dominated by the number of lead ions diffused from the bulk solution to the surfaces of the beads in this case. Based on the Fickian diffusion law, Zhang and Bai [16] showed that the amount of adsorption by diffusion-controlled dynamics as a function of time can be given as:

$$q(t) = 2C_0 S\sqrt{Dt/\pi} = k_d t^{0.5} \qquad (7)$$

where *q(t)* represents the amount of lead ions adsorbed per unit weight of the beads at time t (mg/g), C_0 the initial concentration of lead ions in the bulk solution, *D* the diffusion coefficient, and *S* the specific surface area of the chitosan-cellulose or the crosslinked chitosan-cellulose beads. Eq.(7) indicates that under diffusion-controlled transport mechanism, *q(t)* versus $t^{0.5}$ would follow a linear relationship, with $k_d = 2C_0 S\sqrt{D/\pi}$ depicting the intrinsic kinetic rate constant for diffusion-controlled adsorption.

Fig.8 shows a plot of *q(t)* versus $t^{0.5}$ for the experimental results in Fig.7. A linear relationship of *q(t)* against $t^{0.5}$ is indeed observed in the initial step of adsorption for each type of the beads. The results confirm the existence and importance of diffusion-controlled transport mechanism in lead adsorption on the chitosan-cellulose or crosslinked chitosan-cellulose beads.

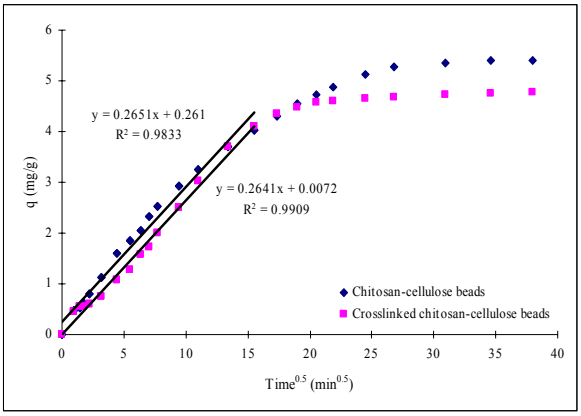

Figure 8 The fitting of diffusion-controlled kinetic model, Eq.(7), to the dynamic adsorption amounts of lead ions for the experimental results in Fig.7

In the later stage of lead adsorption, the experimental data in Fig.7 no longer obey the model in Eq.(7). This indicates that other factors started to play an important role in controlling the adsorption. Since most of the adsorption sites on the beads' surfaces were occupied by previously adsorbed lead ions, the lead ions that were subsequently transported to the surfaces of the beads had to find available adsorption sites before the attachment can occur. The adsorption of lead ions on the beads in the later stage hence slowed down and would probably transit from the initial diffusion-controlled process to a final attachment-controlled process.

3.5 Adsorption mechanisms

X-ray photoelectron spectroscopy (XPS) was employed to investigate the adsorption mechanisms. XPS spectra have widely been used to identify the existence of a particular element and to distinguish the different forms of the same element in a material [4,14,16,19,20]. Fig.9 shows the typical XPS wide scan spectra for the crosslinked chitosan-cellulose beads before and after lead ion adsorption. It is clear that a new peak at the binding energy (BE) of about 136 eV appeared after lead adsorption, and the presence of a satellite band nearby were representative of the oxidation state +2 of lead ions for the pb 4f orbital. Therefore, the peak at BE of 136 eV provides evidence of lead ions (pb^{2+}) being adsorbed on the surface of the beads.

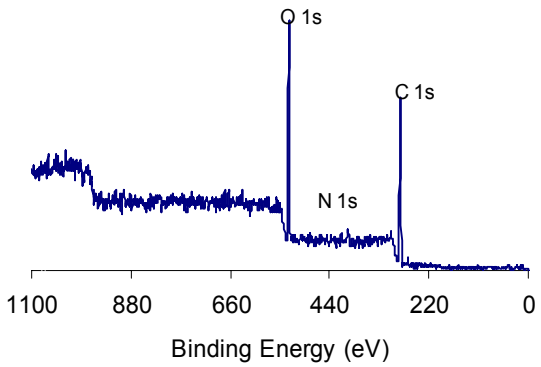

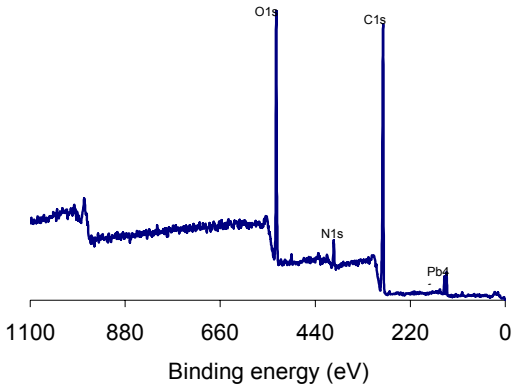

Figure 9 Typical wide scan XPS spectra for the crosslinked chitosan-cellulose beads before and after lead ion adsorption: (a) Before lead adsorption, (b) After lead adsorption

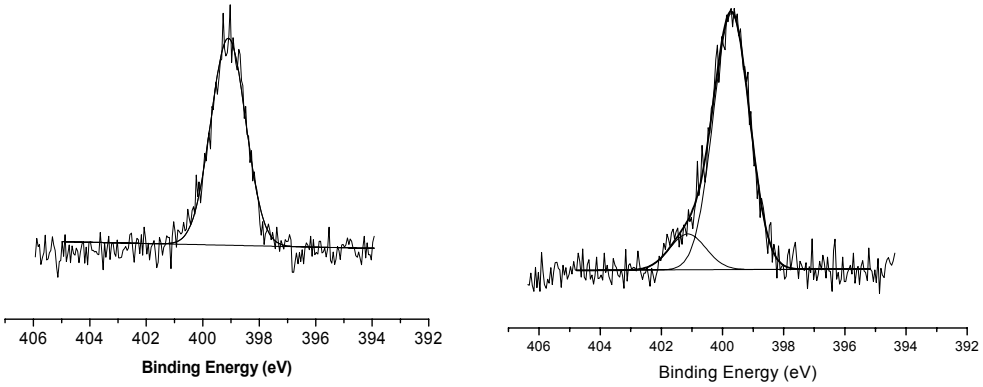

Figure 11 Typical N 1s XPS spectra for crosslinked chitosan-cellulose beads before (left) and after (right) lead ion adsorption

XPS analysis shows that the mechanism of lead adsorption for chitosan-cellulose beads and crosslinked chitosan-cellulose beads are similar. In Fig.10, the typical N 1s XPS spectra of the crosslinked chitosan-cellulose beads before and after lead adsorption are presented, respectively. Before lead ion adsorption, there is only one peak at 399.3 eV for the crosslinked chitosan-cellulose beads. This is attributed to the N atom in the $–NH_2$ and/or the –NH– groups on the surfaces of the chitosan-cellulose or crosslinked chitosan-cellulose beads [16]. After lead ion adsorption, however, a new peak at BE of 401.1eV for the crosslinked chitosan-cellulose beads is observed. This indicates that some N atoms existed in a more oxidized state on the beads' surfaces due to lead ion adsorption. This phenomenon can be attributed to the formation of $R\text{-}NH_2Pb^{2+}$ complexes, in which a lone pair of electrons in the nitrogen atom was donated to the shared bond between the N and Pb^{2+}, and, as a consequence, the electron cloud density of the nitrogen atom was reduced, resulting in a higher BE peak observed. Therefore, the XPS spectra provide evidence of lead

ions binding to nitrogen atoms. The O 1s XPS spectra however did not clearly show significant changes of the O 1s BEs before and after lead adsorption (less than 0.5 eV and the results not shown). Since XPS spectra could not provide clear evidence that the chemical bonds associated with the oxygen atoms on both type of the beads were significantly changed after lead ion adsorption, it may be speculated that the contribution of lead-oxygen interaction to lead ion adsorption on the beads was mainly through a non-specific interaction (physical adsorption, electrostatic attraction, etc.) or a very weak chemical interaction.

4. Conclusion

Chitosan-cellulose hydrogel beads can be used as an effective adsorbent for lead ion removal from aqueous solutions. The addition of cellulose into chitosan made the hydrogel beads materially denser and hence mechanical stronger. The crosslinking reaction using EGDE improved the chemical stability of the chitosan-cellulose beads in acid solutions with pH down to 1. Both the chitosan-cellulose and the crosslinked chitosan-cellulose beads had high adsorption capacities for lead adsorption, although the adsorption performance was pH-dependent (showed maximum adsorption at pH around neutral) and the crosslinked beads had slightly lower adsorption capacities. Freundlich isotherm model can be well fitted for the crosslinked chitosan-cellulose beads and chitosan-cellulose beads. Lead adsorption on both the chitosan-cellulose and the crosslinked chitosan-cellulose beads is found to obey a transport-controlled adsorption kinetics in the initial stage but may transit to an attachment-controlled adsorption kinetics in the later stage. XPS analyses clearly reveal that the nitrogen atoms in chitosan were the main binding sites for lead ions to form surface complexes during the adsorption.

Acknowledgement

The financial support of the Academic Research Funds, National University of Singapore, is acknowledged.

References

[1]. R. Schmuhl, H.M. Krieg and K. Keizer, Water SA 27 (2001) 1.
[2]. J.C.Y. Ng, W.H. Cheung and G. McKay, J. Colloid Interface Sci. 255 (2002) 64.
[3]. G. Bayrammoglu, A. Denizli, S. Sektas, M.Y. Arica and Microchem. J. 72 (2002) 63.
[4]. L. Jin and R.B. Bai, Langmuir 18 (2002) 9765.
[5]. M. Jansson-Charrier, E. Guibal, J. Roussy, B Delanghe and P. Le Cloirec, Water Res. 30 (1996) 465.
[6]. W.S. Wan Ngah, C.S. Endud and R. Mayanar, React. Funct. Polym. 50 (2002) 181.
[7]. J.R. Evans, W.G. David, J.D. MacRae and A. Amirbahman, Water Res. 36 (2002) 3219.
[8]. C.L. Lasko and M.P. Hurst, Environ. Sci. Technol. 33 (1999) 3622.
[9]. S.T Lee, F.L. Mi, Y.J. Shen and S.S. Shyu, Polymer 42 (2001) 1879.
[10]. E. Piron and A. Domard, Int. J. Biol. Macromol. 22 (1998), 33.
[11]. C. Milot, J. McBrien, S. Allen and E. Guibal, J. Appl. Polym. Sci. 68 (1998) 571.
[12]. L. Yang, W.W Hsiao and P. Chen, J. Membrane Sci. 5084 (2001) 1.
[13]. R.B. Bai and C. Tien, J. Colloid Interface Sci. 218 (1999) 488.
[14]. R.B. Bai and X. Zhang, J. Colloid Interface Sci. 243 (2001) 52.
[15]. G.A.F. Roberts (Ed.), Chitin Chemistry, Macmiilan, London, 1992, Chapter 7.
[16]. X. Zhang and R.B. Bai, J. Colloid Interface Sci. 264 (2003) 30.
[17]. Y.A. Ho and G. McKay, Process Biochem. 34 (1999) 451.
[18]. Y. Sağ and Y. Aktay, Biochem. Eng. J. 12 (2002) 143.
[19]. S. Deng and R.B. Bai, Environ. Sci. Technol. 37 (2003) 5799.
[20]. X. Zhang and R.B. Bai, J. Mater. Chem. 12 (2002) 2733.